Impedance Boundary Conditions for the Scattering of Time-Harmonic Waves by Rapidly Varying Surfaces

Jean-René Poirier, Abderrahmane Bendali, and Pierre Borderies

Abstract

A method to build impedance boundary conditions incorporating the effect of rapid variations of a perfectly conducting surface on the scattering of a scalar, E-polarized, time-harmonic electromagnetic wave is presented. The amplitude and the extent of the variations are assumed to be comparable to each other and small as compared to the wavelength. The derivation of the impedance boundary conditions is based on a decomposition of the field in two parts. The first part describes the overall behavior of the wave and the second one deals with its small scale variations. The effective boundary conditions are rigorously constructed for periodic surfaces presenting a large-scale global periodicity to suppress the boundary effects and a small local period to describe the rapid variations. Numerical examples prove that the method can even be heuristically extended to more general problems. In this respect, there are reported some results related to the numerical treatment of small details on a smooth surface and of rough surfaces without resorting to refined meshes.

Index Terms

Electromagnetic Scattering, Impedance Boundary Conditions, Rough Surfaces, Small Details, Homogenization, Periodic Surfaces.

I. Introduction

ADDRESSING electromagnetic scattering by surfaces presenting some rapid variations may be a challenge for numerical methods. An accurate solution requires a very refined mesh which accordingly excessively increases the computational cost. Moreover an excessive overmeshing may induce some numerical locking effects which can damage the approximating properties of the numerical scheme. Such kind of difficulties arise when the scatterer surface presents a localized rapid variation of a small amplitude relatively to the wavelength. In what follows, such variations will be regarded as 'small details'. When the rapid variations spread out along a large part of the surface, 'rough surface' is a more appropriate terminology. However, for the standpoint adopted here, details can be considered as a particular case of rough surfaces. Our objective is thus to reproduce the effect of the rapid variations by means of an effective impedance boundary condition (IBC) obtained through a homogenization process. As a result, it becomes possible again to tackle the solution of the scattering problem by solving a discrete problem of a quite reasonable size. Such boundary conditions are called Leontovitch conditions and are in the form $\mathbf{n} \times (\mathbf{E} \times \mathbf{n}) = Z\,(\mathbf{n} \times \mathbf{H})$ where Z is the equivalent impedance, $\mathbf{E}, \mathbf{H}$ are respectively the electric and the magnetic field and $\mathbf{n}$ is the unit normal to the surface. In the scalar case (2D model), this condition is sometimes referred to as a Fourier-Robin boundary condition and is written $\alpha u + \partial_{\mathbf{n}} u = 0$.

This kind of effective boundary conditions was also proposed for a long time to incorporate the effect of a thin coating in the scattering of electromagnetic waves by a perfectly conducting obstacle (cf., e.g., [1], [2], [3], [4], [5]). Concerning the rough surfaces, Senior [4], [6] has developed an IBC which takes into account a statistically uniform roughness. However, the rapidly oscillating surfaces, considered in this work, are unfortunately outside the range of validity of this approach. Our aim in the present paper is precisely to introduce an appropriate IBC and to prove its efficiency in some applications concerning the treatment of small details and rough surfaces.

In section II, we present an adaptation of the techniques developed in [7] to determine a two-scale asymptotic expansion of the total wave. In particular, we show how this expansion can be used to build a first-order IBC, written on a flat surface and involving slowly varying coefficients only. Then we shortly describe the numerical schemes used to solve the problems respectivey related to the highly oscillating exact surface and to the flat approximate one. The results for the exact surface will be used as a reference solution to test the domain of validity of the homogenization procedure. In section II-B, we apply the IBC approach to uniformly periodic surfaces. Such a kind of surfaces constitutes a particular case of the theory. It makes it possible to measure the accuracy of the homogenization process in terms of some well-defined parameters such as the amplitude, the period or the shape characterizing the variations of the surface. In section III, we use the theory in its full form to deal with two-scale surfaces. The method is then heuristically adapted to include the treatment of both small details in section IV and multiscale random rough surfaces in section V.

Manuscript received Month XX, 2004; revised Month XX, 200X.

J.-R. Poirier is with ENSEEIHT-LEN7, 2 rue Charles Camichel, BP 7122, 31071 Toulouse Cedex 7, France.
A. Bendali is with Laboratoire MIP INSA and CERFACS, 31077 Toulouse Cedex 4, France.
P. Borderies is with ONERA-DEMR, 31055 Toulouse Cedex 5, France.

II. THEORETICAL ASPECTS

A. The two-scale model

We begin with the description of the surfaces that can be considered within the framework of the present theory. A sample of the surface is selected and reproduced by periodicity as depicted in Fig. 1. This is a classical way to proceed (cf., e.g., [8], [9]) used, for example, in the small perturbation method. The sample of the surface of period L and its attached cell are

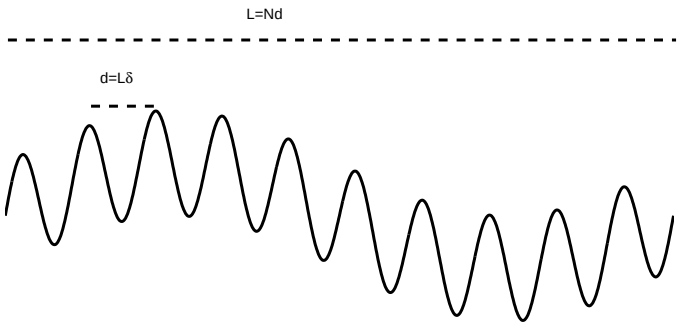

Fig. 1. Finite profile reproduced periodically

defined as follows

$$\Omega^\delta := \left\{(x,y) \in \mathbb{R}^2 : 0 \le x \le L,\ y > \gamma_\delta(x)\right\}, \quad \Gamma^\delta := \left\{(x,y) \in \mathbb{R}^2 : 0 < x < L,\ \ y = \gamma_\delta(x)\right\}$$

where δ is a given small positive parameter characterizing the small amplitude as well as the rapid variations of the surface. This characterization is expressed by means of a function presenting a two-scale variation

$$y = \gamma_\delta(x) := \delta s(x, x/\delta) = \delta s(x,\sigma)|_{\sigma = x/\delta},$$

where the partial functions $x \to s(x,\bullet)$ and $x \to s(\bullet, x/\delta)$ are respectively a periodic function of period L, describing the slow change in the shape of the surface, and a periodic function of period $d = \delta L$, accounting for the oscillations assumed to be fast comparatively to the wavelength. For theoretical purposes only, we further assume that $N := L/d = 1/\delta$ is an integer so that the two-scale function $x \to \gamma_\delta(x)$ is indeed globally periodic of period L. The surfaces so considered present two-scale variations, slow and fast. The amplitude of the variations of the surface is comparable with the period of the fast oscillations.

Implicitly, the function $s(x,\sigma)$ is supposed to be sufficiently derivable with respect to the two variables x and σ. Such an amount of regularity clearly does not match most of the applications, even those considered in section IV in this work. However, it can be considered as a convenient framework providing a theoretical basis for the homogenization process that is subsequently built. It is a quite common practice to make such regularity assumptions in theoretical convergence studies (see, for instance [10]).

We focus on the E-polarized case, that is, on a two-dimensional time-harmonic wave where the electric field is completely characterized by a unique component u^δ. This component completely describes the total wave, assumed to be induced by an incident plane wave u^{inc} defined in the same way. Any plane wave, $u_0 \exp(ik_x x + ik_y y)$, where k_x and k_y are related to the wavenumber by $k = \sqrt{k_x^2 + k_y^2} > 0$, can be considered as a k_x-quasi-periodic function of period L in the variable x. Recall that a function $x \to w(x)$ is k_x-quasi-periodic of period L if the following property holds

$$w(x+L) = e^{ik_x L} w(x), \quad \text{for all } x \in \mathbb{R}.$$

As a result, the total wave u^δ can also be assumed to be k_x-quasi-periodic of period L as a function of x and satisfies the following boundary-value problem for the Helmholtz equation

$$\begin{cases} \Delta u^\delta + k^2 u^\delta = 0 \ \text{ in } \ \Omega^\delta, \\ u^\delta = 0 \ \text{ on } \ \Gamma^\delta, \\ \text{(outgoing) Radiation Condition (RC) on } \ u - u^{\text{inc}}. \end{cases} \tag{1}$$

The radiation condition is the classical quasi-periodic one (cf., e.g., [11], [12]) expressed from the Floquet series expansions of the scattered wave [13].

B. The two-scale asymptotic expansion

1) The two-scale decomposition of the field: An approach, which applies to several kinds of partial differential equations, has been developed in [7]. It consists in seeking a decomposition of the solution as a sum of two functions, respectively depending on a slow and a fast variable, destined to respectively handle the overall behavior of the solution, far enough from

the boundary, and its rapid variations, significant in a thin layer near the boundary only. In this work, we decompose the total wave u^δ as follows

$$u^\delta(x,y) = U^\delta(x,y) + \Pi^\delta(x,\sigma,\tau)|_{\sigma=x/\delta,\ \tau=y/\delta}. \tag{2}$$

For each fixed x, $(\sigma,\tau) \to \Pi^\delta(x,\sigma,\tau)$, defined as a function of (σ,τ) on the elementary cell D,

$$D := \left\{(\sigma,\tau) \in \mathbb{R}^2 : 0 < \sigma < d,\ \tau > s(x,\sigma)\right\},$$

is implicitly assumed to be the restriction to D of a periodic function in σ of period d. The local elementary cell D is depending on x implicitly. The function Π^δ is a boundary layer corrector vanishing as well as any of its derivatives as $\tau \to \infty$. Physically, $\Pi^\delta(x,\sigma,\tau)$ corresponds to evanescent modes generated by the fast oscillations described by the periodicity of the surface in $\sigma = x/\delta$. The fast variable $\tau := y/\delta$ is used to represent the rapid decrease of these modes along the y-axis. As this is seen below, the dependence of $\Pi^\delta(x,\sigma,\tau)$ on the slow variable x is not only destined to fit the low variations of the surface but is also induced by a phase term characterizing the L-periodicity. The variable x of Π^δ plays the role of a parameter in the local problem set in terms of the fast variables (σ,τ).

The overall behaviour of u^δ, far enough from the surface, is described by $U^\delta(x,y)$, a function depending on the slow variables x and y only. Similarly to u^δ, U^δ is supposed to be k_x-pseudo-periodic of period L but is defined on

$$\Omega := \left\{(x,y) \in \mathbb{R}^2 : 0 < x < L,\ y > 0\right\}.$$

As a motivation of such a decomposition, it is sufficient to consider the form of a single fast evanescent Floquet mode for an uniformly periodic surface. A general Floquet mode of order p can be written as follows

$$\Phi_p(x,y) = e^{i\gamma_p x} e^{i\sqrt{k^2-\gamma_p^2}\,y}.$$

with $\gamma_p = k_x + 2\pi p/d$. For p sufficiently large, that is, a fast evanescent mode, Φ_p can be approximated by

$$\Phi_p(x,y) \approx e^{ik_x x} e^{i\frac{2\pi p}{d}x} e^{-\frac{2\pi p}{d}y}.$$

In terms of the large period $L := d/\delta$, this can be also written as a function of x, σ and τ

$$\Phi_p(x,y) \approx e^{ik_x x} e^{i\frac{2\pi}{L}\sigma} e^{-\frac{2\pi}{L}\tau} = \phi_p(x,\sigma,\tau).$$

2) The two-scale asymptotic expansion: Each term of the decomposition (2) is expanded as follows

$$U^\delta(x,y) = \sum_{n=0}^{\infty} \delta^n u^n(x,y), \quad \Pi^\delta(x,\sigma,\tau) = \sum_{n=0}^{\infty} \delta^n \Pi^n(x,\sigma,\tau). \tag{3}$$

The determination of the first few terms of these asymptotic expansions as in [14] will be used to construct a process permitting the computation of an accurate approximation of u^δ much more easily than by solving the problem (1) directly. Actually, the two-scale asymptotic expansion presented here can also be obtained by the technique of correctors [5]. However, the present approach constitutes a more simple and systematic procedure which, at the same time, provides a better insight into the approximation process.

3) Interior equations: Insert (2) and (3) in the Helmholtz equation $\Delta u^\delta + k^2 u^\delta = 0$. The chain rule yields

$$\Delta\Pi^\delta(x,x/\delta,y/\delta) = \left(\delta^{-2}\Delta_{\sigma,\tau}\Pi^\delta + 2\delta^{-1}\partial_x\partial_\sigma\Pi^\delta + \partial_x^2\Pi^\delta\right)(x,\sigma,\tau)|_{\sigma=x/\delta,\ \tau=y/\delta}$$

leading to

$$\left\{\begin{array}{l} \delta^{-2}(\Delta_{\sigma,\tau}\Pi^0) + \delta^{-1}(\Delta_{\sigma,\tau}\Pi^1 + 2\partial_x\partial_\sigma\Pi^0) + \\ \quad \sum\limits_{n\geq 2} \delta^{n-2}(\Delta_{\sigma,\tau}\Pi^n + 2\partial_x\partial_\sigma\Pi^{n-1} + \partial_x^2\Pi^{n-2} + k^2\Pi^{n-2} + (\Delta+k^2)u^{n-2}) = 0. \end{array}\right. \tag{4}$$

Equating to zero the coefficient of any power of δ in (4), we get

$$\left(\Delta_{\sigma,\tau}\Pi^n + 2\partial_x\partial_\sigma\Pi^{n-1} + \left(\partial_x^2 + k^2\right)\Pi^{n-2}\right)(x,\sigma,\tau) + \left(\Delta u^n + k^2 u^n\right)(x,y) = 0.$$

The condition on Π^δ, for $\tau \to \infty$ that expresses that Π^δ represents evanescent modes, uncouples u^n and Π^n, yielding for u^n

$$\left\{\begin{array}{l} \Delta u^n + k^2 u^n = 0 \text{ in } \Omega \\ \text{RC on } u^0 - u^{\text{inc}} \text{ and on } u^n, \end{array}\right. \tag{5}$$

and for the first two terms Π^0 and Π^1

$$\left\{\begin{array}{l} \Delta_{\sigma,\tau}\Pi^0 = 0 \text{ and } \Delta_{\sigma,\tau}\Pi^1 + 2\partial_x\partial_\sigma\Pi^0 = 0 \text{ in } D, \\ \lim\limits_{\tau\to\infty} \Pi^0(x,\sigma,\tau) = 0, \quad \lim\limits_{\tau\to\infty} \Pi^1(x,\sigma,\tau) = 0. \end{array}\right. \tag{6}$$

System (6), satisfied by Π^0 and Π^1, has to be regarded as a family of systems depending smoothly on the parameter x. However, as it will be shown below in the implementation of the method, only a limited number of such systems are really solved.

4) Equations resulting from the boundary condition: Plug (2) and (3) in the boundary condition. Up to and including the terms in δ, this can be written

$$u^0(x,\delta s(x,\sigma)) + \Pi^0(x,\sigma,s(x,\sigma)) + \delta(u^1(x,\delta s(x,\sigma)) + \Pi^1(x,\sigma,s(x,\sigma))) = \mathcal{O}(\delta^2).$$

Discarding once more all the terms in δ^2 and using a Taylor expansion in y, we get an approximate expression for the boundary condition, explicit relatively to the parameter δ,

$$u^0(x,0) + \Pi^0(x,\sigma,s(x,\sigma)) + \delta(s(x,\sigma)\partial_y u^0(x,0) + u^1(x,0) + \Pi^1(x,\sigma,s(x,\sigma)) = 0.$$

Again, equating to 0 the constant term in δ as well as the coefficient of δ in the above condition, we are led to the following system

$$\left\{ \begin{array}{l} \Pi^0(x,\sigma,s(x,\sigma)) + u^0(x,0) = 0 \\ \Pi^1(x,\sigma,s(x,\sigma)) + s(x,\sigma)\partial_y u^0(x,0) + u^1(x,0) = 0 \end{array} \right. \tag{7}$$

Systems (5) and (6) are thus coupled by the boundary condition (7).

In (5), the slow variable "does not see" the rough surface. The equations are posed in the domain Ω with the flat boundary $\Gamma := \big\{(x,0) \in \mathbb{R}^2 : 0 < x < L\big\}$.

C. Determination of the first order terms

We limit the determination of the asymptotic expansion to the lowest order terms that are involved in the construction of the impedance boundary condition used below, that is, u^0, u^1, Π^0 and Π^1.

The problem satisfied by Π^0 has the following statement

$$\left\{ \begin{array}{l} \Delta_{\sigma,\tau}\Pi^0 = 0 \text{ in } D, \\ \Pi^0(x,\sigma,s(x,\sigma)) + u^0(x,0) = 0. \end{array} \right. \tag{8}$$

It can be proved [15] that $\Pi^0(x,\sigma,\tau)$ is constant, as a function of (σ,τ), and that it is uniquely determined. As it vanishes for $\tau \to \infty$, $\Pi^0(x,\sigma,\tau) = 0$ so that $u^0(x,0) = 0$. We have thus established that the crudest approximation of the solution is simply obtained by solving the problem on the mean flat surface, without having to take any limit as $\delta \to 0$. In other words, the roughness is not seen at order 0

$$\left\{ \begin{array}{l} \Delta u^0 + k^2 u^0 = 0 \text{ in } \Omega, \\ u^0(x,0) = 0, \\ \text{RC on } u^0 - u^{\text{inc}}. \end{array} \right.$$

Now, we come to the determination of the first-order term. First, we gather the conditions satisfied by Π^1

$$\left\{ \begin{array}{l} \Delta_{\sigma,\tau}\Pi^1 = 0 \text{ in } D, \\ \Pi^1(x,\sigma,s(x,\sigma)) + s(x,\sigma)\partial_y u^0(x,0) + u^1(x,0) = 0, \\ \lim\limits_{\tau\to\infty} \Pi^1(x,\sigma,\tau) = 0. \end{array} \right. \tag{9}$$

In (9), variable x plays the role of a fixed parameter. To construct a function Π^1 satisfying (9), we first introduce the auxiliary problem

$$\left\{ \begin{array}{l} \Delta_{\sigma,\tau}\alpha = 0 \text{ in } D, \\ \alpha(x,\sigma,s(x,\sigma)) = s(x,\sigma), \\ \alpha \text{ bounded as } \tau \to +\infty. \end{array} \right. \tag{10}$$

which has one and only one solution α depending smoothly on x as this was established in [15]. In view of the two first equations of (9), Π^1 is necessary in the form

$$\Pi^1(x,\sigma,\tau) = -\alpha(x,\sigma,\tau)\partial_y u^0(x,0) - u^1(x,0) \tag{11}$$

It was also established in [15] that

$$h(x) = \lim_{\tau\to\infty} \alpha(x,\sigma,\tau).$$

Finally, the third condition in (9), $\lim_{\tau\to\infty} \Pi^1(x,\sigma,\tau) = 0$ determines the boundary condition reducing with (11) the determination of u^1 to the solution of the following problem

$$\left\{ \begin{array}{l} \Delta u^1 + k^2 u^1 = 0 \text{ in } \Omega, \\ u^1(x,0) + h(x)\partial_y u^0(x,0) = 0, \\ \text{RC on } u^1. \end{array} \right.$$

D. Construction of the impedance boundary condition

Instead of solving two boundary-value problems to determine $u^0 + \delta u^1$, it is more convenient to construct an equivalent impedance boundary condition on the flat surface leading to a boundary-value problem whose solution gives an approximation $\widetilde{u}^\delta = u^0 + \delta u^1 + \mathcal{O}(\delta^2)$ including the zero and first order terms.

The construction starts from the following simple observation. The truncated expansion $u^0 + \delta u^1$ satisfies the Helmholtz equation as well as the radiation condition. It is indeed possible to write an explicit boundary condition for $u^0 + \delta u^1$ satisfied up to a term in δ^2. More precisely, in view of the above conditions, satisfied respectively by $u^0(x,0)$ and $u^1(x,0) + h(x)\partial_y u^0(x,0)$, we have

$$\big(u^0(x,0) + \delta u^1(x,0)\big) + \delta h(x)\partial_y \big(u^0(x,0) + \delta u^1(x,0)\big) = \delta^2 h(x)\partial_y u^1(x,0).$$

Neglecting the term in δ^2, we are led to the homogenized problem, related to an impedance boundary condition, which is actually solved in order to determine $\widetilde{u}^\delta$

$$\begin{cases} \Delta\widetilde{u}^\delta + k^2\widetilde{u}^\delta = 0 \text{ in } \Omega, \\ \widetilde{u}^\delta(x,0) + \delta h(x)\partial_y\widetilde{u}^\delta(x,0) = 0, \\ \text{RC on } \widetilde{u}^\delta - u^{\text{inc}}. \end{cases} \tag{12}$$

Recall that $h(x)$ is obtained from the solution of the local problem (10) for each value of x.

E. Numerical solution of the exact and the impedance boundary-value problems for periodic surfaces

An adaptation of the Finite Element Method (FEM) to problems involving a periodic boundary condition, known as periodic FEM (cf., [16], [15], [17]) is used to solve problem (1) numerically on a very refined mesh. The obtained solution is used as a reference solution to test the domain of validity of the homogenization procedure.

The periodic FEM is also used to determine an approximate value for the coefficient $h(x)$ of the IBC by solving the corresponding boundary-value problem (10).

Problem (12) on the flat boundary is solved by a collocation method. Its solution is expanded in Floquet modes whose coefficients are determined by enforcing the IBC at $\{y = 0\}$.

Two solutions u_1 and u_2 are compared by means of the following energy error

$$e_2 = \sum_{n=-N}^{N} |u_{1,n} - u_{2,n}|^2 \tag{13}$$

where $u_{1,n}$ and $u_{2,n}$ stand for the coefficients of their respective propagative Floquet modes.

III. Periodic surfaces

A. Uniformly periodic surfaces

1) Homogenization of uniformly periodic surfaces: We first consider uniformly periodic surfaces, that is, surfaces described by a function $(x,\sigma) \to s(x,\sigma)$ which is constant in x. This particular case is of course within the scope of the above theory. Special features make this example particularly suited to check the validity of the homogenization procedure. First, the exact problem can be solved accurately on one small cell only. Furthermore, as the period d of the surface is assumed to be small as compared to the wavelength λ, only the fundamental Floquet's mode is propagative. Hence, immediately above the surface roughness, the total field admits the following decomposition

$$u^\delta(x,y) = u^{\text{inc}}(x,y) + R_0 e^{i(k_x x + k_y y)} + \text{ evanescent terms.}$$

Problem (12) can be solved for any multiple L of d and in particular for $L = d$. Its solution is completely characterized by R_0 which can be viewed as the reflection coefficient of the incident wave.

Fig. 2. Periodic surfaces: sine, step and triangular shaped

Fig. 3. Periodic surfaces: high step, positive sine, sine in absolute value

2) IBC computation: The various shapes of the unit cell, that are considered, are depicted in Fig. 2 and Fig. 3 respectively. We first examine how $h = h(x) = \lim_{\tau \to \infty} \alpha(\sigma, \tau)$ depends on the size and on the shape of the elementary cell.

Since the surface is metallic, the modulus of the reflection coefficient is of course equal to 1. For the six geometric shapes given in Fig. 2 and Fig. 3, all the cells have a same maximum height h_0. Actually, only the ratio d/h_0 is relevant. By decreasing this ratio from 1 to some small value ε, we can consider a geometry which becomes more and more oscillating.

The variation of h as a function of the cell size for the six cell shapes is plotted in Fig. 4. Recall that the results do not depend on frequency as mentioned above provided the size of the cell D remains small compared to the wavelength. Some observations can be carried out.

- For a highly oscillating surface (that is, as the period tends to zero), h tends to a maximum value $h_{\max}$ close to the maximum height h_0 of the ruggedness.
- The slower the oscillations are, the deeper the penetration of the wave is.
- The larger the period of the elementary cell is, the better the underneath geometry becomes visible by the incident wave.

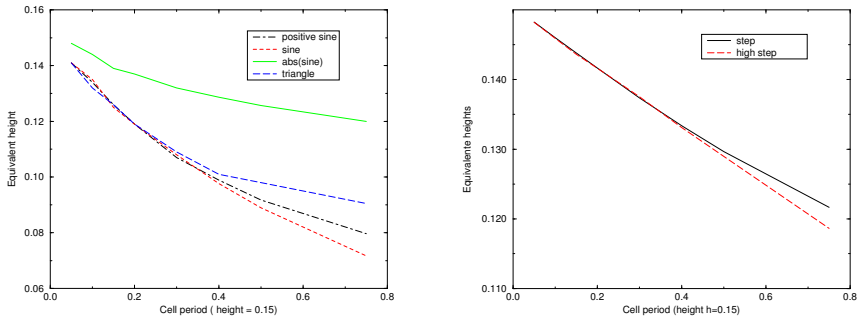

Fig. 4. Equivalent heights as a function of the cell period

3) The scattering problem solution: The reflected wave corresponding to the effective IBC in problem (12) is a plane wave $R\, e^{i(k_x x + k_y y)}$ completely expressed by means of the reflection coefficient

$$R := -\frac{1 + ik_y h\delta}{1 - ik_y h\delta}.$$

Comparison of R and the coefficient R_0 relative to the reference solution gives a precise handling of the error induced by the homogenization process. Since both $|R|$ and $|R_0|$ are equal to 1, the approximation of R_0 by R is more adequately measured in terms of their phase angle.

In Fig. 5, we have plotted the phase angles of R_0 and R versus the angle of incidence of the incident wave for the sine shape and for various values of d expressed in units of wavelength. Three conclusions can be drawn.

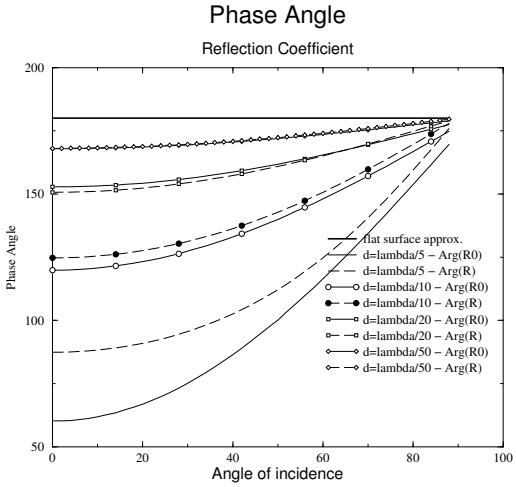

Fig. 5. Phase angle of the reflection coefficient versus the angle of incidence for the sine profile

- Accurate results are obtained for $d = \lambda/20$, and with an acceptable error for $d = \lambda/10$.
- The results are more accurate for oblique than for normal incidences.
- Even beyond the validity range of the method related to an error that can be reasonably accepted, that is, for $d > \lambda/5$, the homogenization process continues to give better results than the approximation by a flat plate in a significant way.

Remark and interpretation. Due to the uniqueness of the solution to problem (10), posed in the elementary cell, $h(x)$ is necessarily real. Let us consider the reflection of the incident wave by the plane $\{y = h\delta\}$: the reflected wave is then $R_{\text{eq}} e^{i(k_x x + k_y y)}$ with

$$R_{\text{eq}} := -e^{2ik_y h\delta} = R + \mathcal{O}(\delta^2).$$

The reflection coefficients R and R_{eq} are equal up to a term in δ^2. The parameter $h(x)$ can hence be regarded as a normalized slowly variable height which takes into account the fast variations of surface on the scattering of the incident wave.

4) Homogenization versus refined sampling : We compare the accuracy of the results delivered by the homogenization process with those obtained directly by solving on meshes of various size. The reference solution is still the one obtained above on a very refined mesh. The respective errors for the sine shape, defined as in (13), are plotted in Fig. 6. We consider a sine shape whose amplitude and period are equal. The following values $d = \lambda/10$ and $d = \lambda/20$ were successively considered.

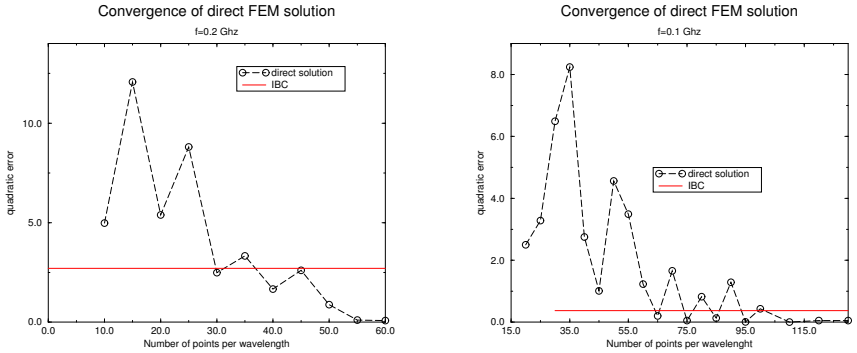

Fig. 6. Sine of height $\lambda/10$ and $\lambda/20$

Three features can be pointed out.

- The direct computation requires 40 points per wavelength and 100 points per wavelength respectively to yield the same accuracy than the homogenization process.
- As it has been already observed, the IBC approach begins to deliver accurate results at $d = \lambda/10$. The error in the phase is then less than 5 degrees.
- Better accuracy can be observed for a roughness of a smaller thickness.

Now, we address the approximation delivered by the IBC for sine shapes having the same amplitude $\lambda/10$ and various periods. The results are reported in Table I including those for the flat plate.

Period	$\lambda/30$	0.1λ	0.2λ	0.3λ	0.4λ	0.5λ	0.875λ
Flat surf.	67.5°	60.2°	51.1°	43.5°	36.9°	30.9 °	11.6°
IBC	6.5°	4.7°	2.7°	1.0°	0.7°	2.4°	11.°

TABLE I
ERROR FOR A FIXED AMPLITUDE AND A VARYING PERIOD

Results obtained using IBC are in good agreement with the reference solution for periods up to $\lambda/3$. This is obviously beyond the expected domain of validity of the method.

B. Two-scale periodic surfaces

1) Numerical solution of the scattering problem: A simple two-scale periodic surface can be obtained by adding to the fast oscillations of an uniformly periodic surface a slow variation term. More precisely, the shape is obtained as a superposition of two sine functions, with respectively a large period L, of several wavelengths, and a short period d, small compared to the wavelength (Fig. 7). The effective condition now depends on the slow variable x. As an example, we consider a surface with a large period $L = 8\lambda$, λ being the wavelength, a small period $d = \lambda/10$, and an amplitude $\lambda/10$.

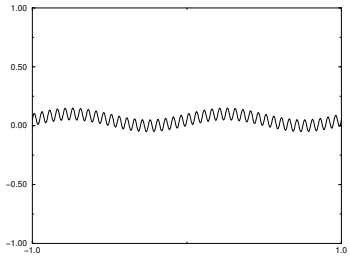

Fig. 7. The two-scale periodic surface

Since the IBC solution handles propagative modes only, the field is computed sufficiently far from the surface, at a sufficiently large height h_∞, so that no evanescent mode contributes to the direct reference solution there. Practically, it is sufficient to take a few wavelengths. In Fig. 8, we have plotted the modulus and the phase angle over a period for three computations:

1) the reference solution computed on a mesh of 100 nodes per wavelength,
2) the FEM direct solution obtained with a coarse mesh of 10 nodes per λ only, clearly not sufficient to represent the surface correctly,
3) the collocation solution obtained through an IBC computed using a coarser mesh of 5 nodes per λ on the plane surface $\{y = 0\}$. The reported tests have been achieved using an incident plane wave at normal incidence.

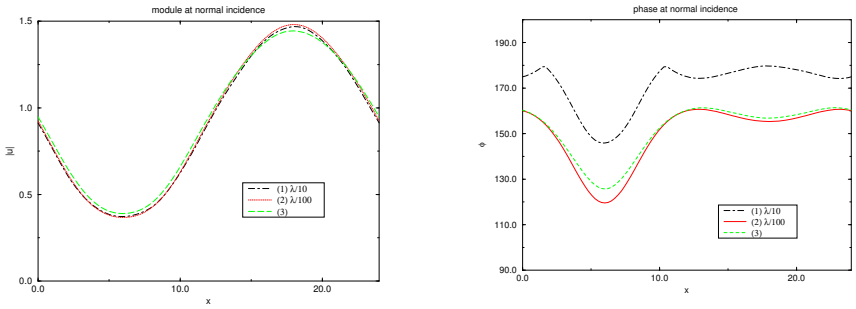

Fig. 8. (1) Direct solution at $\lambda/10$, (2) reference at $\lambda/100$, (3) IBC

For the method (2), the error on the modulus is acceptable but is large for the phase. The method (3) produces rather good results both in magnitude and phase.

The same tests have been repeated for an incident wave at 60 degrees. The results are depicted in Fig. 9 and Fig. 10. The modulus relative to the three solutions is plotted in Fig. 9. Although the improvement gained by the IBC can be clearly observed, it is small when compared with the solution obtained on the coarse mesh. By contrast, the error on the phase angle, reported in Fig. 10, clearly brings out the improvement carried out by the IBC.

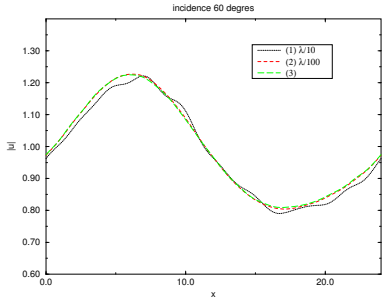

Fig. 9. (1) Direct solution at $\lambda/10$, (2) reference à $\lambda/100$, (3) IBC

Therefore, these tests can be considered as a first numerical validation and a justification of the homogenization process.

2) IBC solution versus direct FEM modeling: When several Floquet modes are propagative, the modulus of the scattered field becomes a parameter as significant as the phase angle. For the following numerical computations, we use (13) again to measure the error resulting from the approximation process.

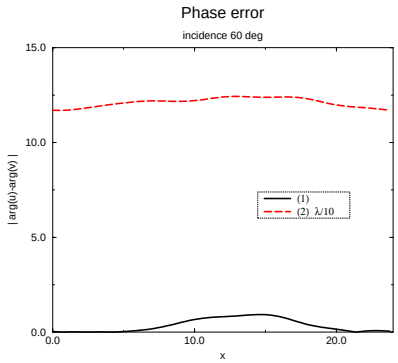

Fig. 10. (1) IBC, (2) Direct solution at $\lambda/10$

We compare the results obtained by the IBC approach with those obtained by directly solving the scattering problem on meshes of various sizes Δx respectively equal to $\lambda/10$, $\lambda/20$ and $\lambda/50$. We have also considered three periodic surfaces whose respective height $h_{\max}$ is equal to $\lambda/20$, $\lambda/10$ and $\lambda/5$.

Δ_x \ h_{max}	$\lambda/5$	$\lambda/10$	$\lambda/20$
$\lambda/10$	32%	43%	
$\lambda/20$	3%	16%	23%
$\lambda/50$		1%	2%
IBC	24%	4%	0.6%

TABLE II
NORMAL INCIDENCE

Δ_x \ h_{max}	$\lambda/5$	$\lambda/10$	$\lambda/20$
$\lambda/10$	23%	20%	
$\lambda/20$	2%	9%	11%
$\lambda/50$		0.6%	1%
IBC	4%	0.4%	0.1%

TABLE III
60 DEGREES INCIDENCE

As reported in table II and table III, the results based on the homogenization process are in good agreement with the reference solution for $h_{\max} \leq \lambda/10$. The accuracy reached by the IBC corresponds to that provided when the scattering problem is solved on a mesh of 50 points per wavelength in a direct fashion. Note that $h_{\max} = \lambda/5$ is beyond the range of validity of the method, thereby explaining the large error of 24% in the results at normal incidence. However, for such a roughness, the error at oblique incidence still remains acceptable.

IV. APPLICATION TO SMALL DETAILS

A. Introduction

Now we turn our attention to the case of a small detail included on a periodic surface of period L (a few wavelengths). This case is not rigorously covered by the previous theoretical framework. But the small size of a detail well matches with the use of a multi-scale method. Here, we propose an heuristic extension that permits the treatment of such a case. In the theoretical model, the local behavior is characterized by a local period d being part of the data. It consists in assembling a number of small cells to form the large cell of size $L = Nd = d/\delta$, as represented in Fig. 11. We now indicate how this can be heuristically extended to the current context.

Clearly, the local period no longer really exists now. The cell of size d that is depicted in Fig. 12 can be understood as a local periodic approximation reproducing the local behavior of the surface.

Fig. 11. Periodic surface with $L = Nd$

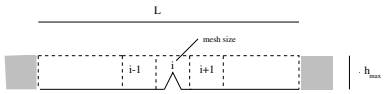

Fig. 12. Detail

From obvious physical considerations, d must be small comparatively to the wavelength. It must also be larger than the mesh size p to avoid any loss of information. These observations, as well as the quantitative results obtained in table I, indicate that d should be approximately equal to $\lambda/3$.

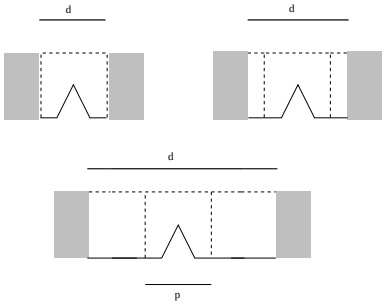

Fig. 13. Various choices for the fictitious local period

Note that the numerical approximation of the scattered wave depends on a second parameter: the mesh size p. It accounts for the slow variations of the surface. Typical size of p is $\lambda/10$ for FEM modelling while d is of the order of $\lambda/3$. The following study will provide a good indication on the way to choose these two parameters.

B. Optimal choice of the local period relatively the geometry

The error on the modulus is measured using (13). The reference solutions u_{ref} are obtained using a very refined mesh (more than 200 points per wavelength, see Fig. 14). The objective is to make the error as small as possible for various shapes of the detail: triangle, crenel and sine, whose size is $\lambda/10 \times \lambda/10$. The incident wave is at normal incidence. To bring out the accuracy that is gained, we plot the solution, obtained with $d = 0$, corresponding to a crude approximation by a flat surface. As expected, the best results correspond to values for d between $\lambda/5$ and $\lambda/2$. Values greater than λ are clearly beyond the

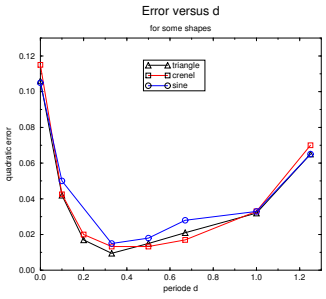

Fig. 14. Behaviour of the error relatively to the local fictitious period for some shapes

range of validity of the approximation. An interesting conclusion is that the choice for the local period d is not at all critical provided it is taken within the indicated range of values.

C. *Optimal choice of the local period relatively to the angle of incidence*

The same tests, as above for the crenel, but with an incident wave at different incidences: 30, 60 and 80 degrees are reported in Fig. 15.

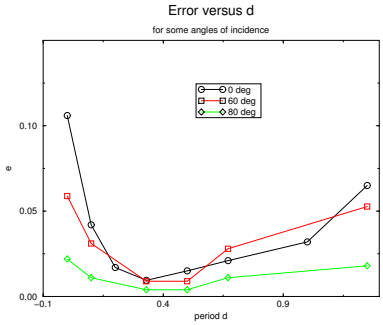

Fig. 15. Behaviour of the error relatively to the local fictitious period for some angles of incidence

As expected the accuracy does not depend on the incidence of the incident wave. So, another interesting feature of this approach is that the error is approximately the same for all angles of incidence.

V. Application to rough surfaces

Since the homogenization process has led to an IBC which is expressed through a differential operator, it makes sense to extend this approach to a general rough surface, at least in a formalist way. Actually, we follow the heuristic approach previously introduced in section IV. We remain within the framework of the two-scale model. The local scale is obtained by windowing the local surface and making it periodic. We then see that a rough approximation is introduced by imposing a periodic boundary condition on the left and the right of the local cells but the remaining part of the derivation of the IBC is undertaken identically. The aim of the following numerical tests is to show that the homogenization process still remains a good approximation procedure.

The test-case being considered here is a multiscale random rough surface highly oscillating. It is generated from the Weierstrass function, whose infinite series is truncated here between 1 and n_2,

$$W(x) = \eta \frac{\sqrt{2}(1 - b^{(2D-4)})^{\frac{1}{2}}}{(b^{(2D-4)} - b^{(2D-4)(n_2+1)})^{\frac{1}{2}}} \sum_{n=1}^{n_2} (\frac{1}{b^{(2-D)n}} cos(2\pi b^n x + \theta_n))$$

where

- D is the fractal dimension parameter, characterizing the roughness which ranges from 1 to 2 to increase the ruggedness,
- θ_n is a random phase,
- η^2 is the maximum variance,
- n_2 is the number of scales being considered,
- b is a positive irrational parameter ($b = \sqrt{\pi}$ here).

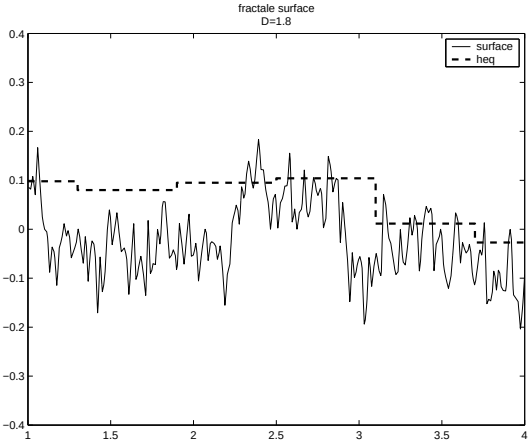

Fig. 16. Multiscale rough surface

A very rough surface is obtained by choosing $D = 1.8$ (see Fig. 16). The root mean square height (rmsh) of the profile are $\lambda/15$ and $\lambda/30$, which corresponds to maximum heights of respectively $\lambda/5$ and $\lambda/10$. We are hence at the limit of validity of the method which has been pointed out previously in the case of periodic surfaces in section II-B. The corresponding sample is represented in Fig. 16 as well as the IBC.

Like in section III, appropriate choice for the local period d has to be done. Its influence is evaluated below. To this end, we use the following procedure.

- Define the IBC as a function constant by element, on an uniform mesh. The related mesh size is denote by p. This mesh is further used to solve the homogenized problem.
- Use a cell, whose size is denoted by d, centered on the element on which the value of the IBC is being computed.

The errors on the results obtained the homogenization process are reported in Table IV for various values of d, p and θ. They are computed as above in terms of (13) using a reference solution computed on a very refined mesh.

An interesting indication on the efficiency of the IBC approach can be brought out by considering the error relative to the crudest approximation by a flat surface. For an incidence of 60 degrees, this error is 18.8 %. It reaches 37.2 % at normal incidence.

p \ d		0.1λ	0.2λ	0.3λ	0.4λ	0.5λ
$\lambda/10$	$\theta = 0^{\circ}$	4.1 %	2.75 %	2.9 %	4.8 %	5.4 %
$\lambda/10$	$\theta = 60^{\circ}$	1.8 %	1.3 %	2 %	3.2 %	4.2 %
$\lambda/5$	$\theta = 0^{\circ}$	4 %	2.85 %	2 %	3.9 %	6.1 %
$\lambda/5$	$\theta = 60^{\circ}$	4.2 %	2.1 %	1.7 %	3.2 %	4.8 %
$\lambda/3$	$\theta = 0^{\circ}$	18.7 %	10.1 %	6.7 %	6.4 %	5.2 %

TABLE IV

ERRORS FOR DIFFERENT MESH SIZES p AND PERIODS d

Table IV provides the last ingredient concerning the strategy of choosing the mesh size p and the cell size d. The best results are obtained with d slightly larger than p. This can be interpreted from the fact that the information contained in the mesh element is then fully used and the side-effect resulting from the fictitious periodic boundary conditions are reduced as much as possible. Note that the quality of the approximation is not very sensitive to this choice as long as d remains small compared to the wavelength. As a result, it is sufficient to use a mesh size of the order $\lambda/5$ or $\lambda/10$ to produce satisfactory results.

A comparison of the homogenized solution with the reference one is depicted in Fig. 17 and Fig. 18. Two lines single out the error for $p = \lambda/5$ and $d = \lambda/3$ and a more accurate solution obtained with $p = \lambda/10$ and $d = \lambda/5$.

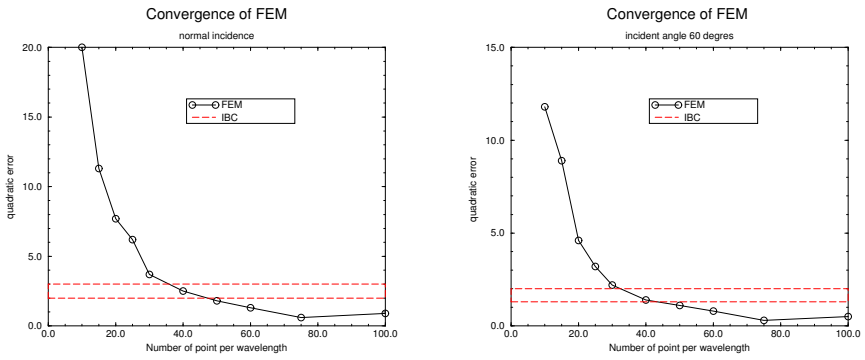

Fig. 17. Random surface D=1.8, rmsh=$\lambda/30$

The results exhibit a good agreement with the reference solution. The accuracy reached is equivalent to that based on a direct solution using 30 to 40 points per wavelength. The size of the problem to be solved is reduced by a factor 6 when using the homogenization approach with $p = \lambda/5$ for this two-dimensional case.

Some results on the approximation of the modulus are reported in Fig. 19 which shows a quite good agreement of the overall behavior of the solution with the reference one.

Similar tests can be found in [15] as well as a description of stochastic surfaces in [18]. The good results, obtained here, suggest that the fictitious periodic condition imposed on the small local cells does not significantly contribute to the overall error induced by both the homogenization and the approximation process which is itself very small. Note that, in this study, we have

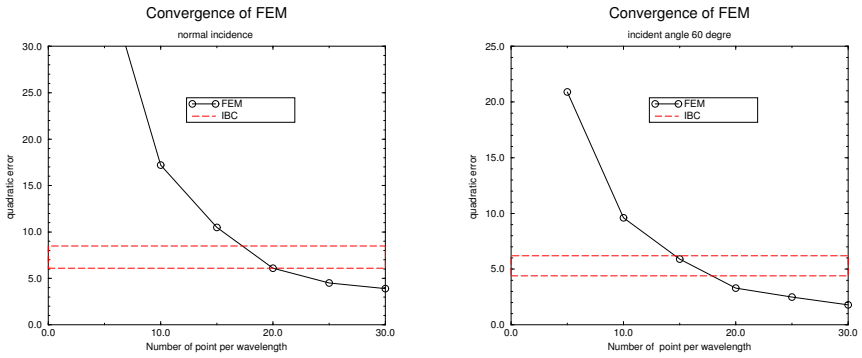

Fig. 18. Random surface D=1.8, rmsh=$\lambda/15$

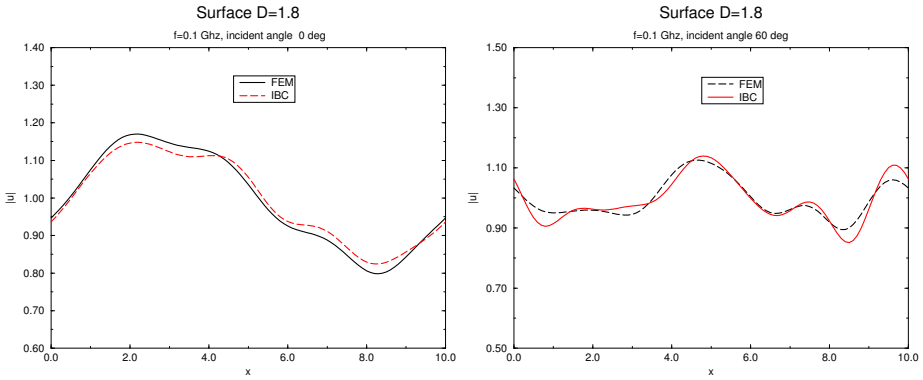

Fig. 19. Modulus of the field, rmsh=$\lambda/30$

only dealt with the construction and the measure of the performance of a procedure to solve the scattering problem numerically without resorting to a very fine sampling of the surface. We have tackled no question concerning the electromagnetic properties of the multiscale random surfaces. This is a large study on its own, demanding large scale computations. One of the motivations of this work, besides making such computations feasible, was precisely to accelerate them.

VI. Conclusion

The theoretical as well as the numerical results of this study have shown the relevance of the homogenization technique in the solution of scattering of waves by a highly oscillating surface. Even if no theoretical foundation is available for non periodic or multiscale surfaces, the approach gives quite good results for these cases too. The present limitations are related to the maximum height of the roughness which must be less than $\lambda/10$. The technique can be improved by using higher-order IBCs. Combined with a numerical method like the Method of Moments (MoM), FEM or FDTD, it can yield an efficient solution technique for scattering and radiation problems involving small details or rough surfaces [19]. It can be combined with a Monte-Carlo process to deal with random rough surfaces as a straightforward application of the homogenization process presented in this work. In this paper, only perfectly conducting surface with TM polarization has been considered. Extension to the other polarization and to the dielectric case should follow the same methodology leading to a transmission instead of a boundary condition. This should yield the transmitted as well as the reflected field. The extension to the three dimensional case has been done theoretically [15] and its full study will be covered in a forthcoming paper.

Acknowledgment

The authors would like to thank the referees for their thorough reading and constructive remarks which have contributed to improve the final appearance of this paper.

References

[1] A. Bendali, M. Fares, and J. Gay, “A boundary-element solution of the leontovitch problem,” *IEEE Trans. Antennas Propagat.*, vol. 47, no. 10, pp. 1597–1605, october 1999.
[2] B. Engquist and J.-C. Nedelec, “Effective boundary conditions for electro-magnetic scattering in thin layers,” Palaiseau, France, 1993.
[3] A. Bendali and K. Lemrabet, “The effect of a thin coating on the scattering of a time harmonic wave for the helmoltz equation,” *SIAM J. Appl. Math.*, vol. 56, no. 6, pp. 1664–1693, Dec. 1996.

[4] T. B. A. Senior and J. L. Volakis, *Approximate boundary conditions in electromagnetics*, ser. 41. London: IEE Electromagnetic waves, 1995.
[5] T. Abboud and H. Ammari, "Diffraction at a curved grating: TM and TE cases, homogenization," *Journal of Mathematical Analysis and Application*, vol. 202, no. 3, pp. 993–1026, 1996.
[6] T. B. A. Senior, "Impedance boundary condition for imperfectly conducting surfaces," *Appl. Sci. Res.*, vol. 8, pp. 418–436, 1960.
[7] A. B. Vasil'eva, V. F. Butuzov, and L. V. Kalachev, *The Boundary Function Method for Singular Perturbation Problems*. Philadelphia: SIAM Studies in Applied Mathematics, 1995.
[8] A. Ishimaru, *Wave propagation and scattering in random media*. New York: IEEE Press, 1997.
[9] J. Ogilvy, *Theory of wave scattering from random rough surfaces*. Bristol: Adam Hilger, 1991.
[10] E. Sánchez-Palencia, "Un problème d'écoulement lent d'un fluide incompressible au travers d'une paroi finement perforée," in *Homogenization methods: theory and applications in physics (Bréau-sans-Nappe, 1983)*. Paris: Eyrolles, 1985, pp. 371–400.
[11] R. Petit, Ed., *Electromagnetic Theory of Grating*, springer-verlag, heidelberg ed. Topics in Current Physics, 1980.
[12] L. Rayleigh, "On the dynamical theory of gratings," *Proc. R. Soc. Lon. A*, vol. 79, pp. 399–416, 1907.
[13] A. F. Peterson, S. L. Ray, and R. Mittra, *Computational Methods for Electromagnetics*, ser. IEEE/OUP Series on Electromagnetic Wave Theory. New York: IEEE Press and Oxford University Press, 1998.
[14] A. G. Belyayev, A. G. Mikheyev, and A. S. Shamayev, "Diffraction of a plane wave by a rapidly oscillating surface," *Comput. Maths. Phys.*, vol. 32, no. 8, pp. 1221–1133, 1992.
[15] J.-R. Poirier, "Modélisation électromagnétique des effets de rugosité surfacique," Ph.D. dissertation, INSA de Toulouse, Dec 2000.
[16] R. R. R. Beck, B. Erdmann, "Kaskade 3.0 an object-oriented adaptive finite element code," Konrad-Zuse-Zentrum fur Informationtechnik Berlin, Tech. Rep. 95-4, 1995.
[17] P. Ferreira, "Etude numérique de quelques problèmes de diffraction d'ondes par des réseaux périodiques en dimension 2," Ph.D. dissertation, Ecole polytechnique, Palaiseau, France, 1998.
[18] J. A. Ogilvy and J. R. Foster, "Rough surfaces:gaussian or exponential statistics," *Appl. Phys.*, vol. 22, no. 9, pp. 1243–1251, Sept 1989.
[19] J.-R. Poirier, A. Bendali, and P. Borderies, "Homogenization techniques for small scale details on a large object," 2002, jEE'02 , Toulouse, France, 1-3 mars 2002.

PLACE PHOTO HERE

Jean-René Poirier received the Engineer diploma from the National Institute of Applied Sciences at Toulouse, France in 1996. He was a Ph.D. student at the The French National Aeronautics and Space Research Centre (ONERA) from 1997 to 2000 and received the Ph.D. degree in applied mathematics from INSA in december 2000. From 2001 to 2003, he joinded the Institute of Analysis and Scientific Computing from EPFL, Lausanne, Switzerland. He is currently working as an associate professor at the electronic laboratory of ENSEEIHT (LEN7), Toulouse, France.

PLACE PHOTO HERE

Abderrahmane Bendali see bendali bio doc

PLACE PHOTO HERE

Pierre Borderies was born in France in 1953. He received the diploma of Engineer from Ecole Superieure d'Electricite, Paris, France in 1975. After a period of teaching in Venezuela, he joined the Centre d'Etudes et de Recherches de Toulouse, part of Office National d'Etudes et de Recherches Arospatiales (CERT-ONERA) in 1979. Since then, he has been working as a research engineer in the micowaves department. He has worked in the fields of large reflector antennas, microwave devices and radar targets imaging, characterisation and identification. In 1990-91, he spent a sabbatical year at New York University, Farmingdale, NY. In 1997, he obtained the universitary grade of Habilitation to Direct Reasearch. His current research interests include radiation and scattering of antennas, frequency selective surfaces, ultra wide band scattering, subsurface targets identification, natural targets scattering and remote sensing.